

Heat and moisture management for automatic air conditioning of a domestic household using FA-ZnO nanocomposite as smart sensing material

Article

Published Version

Creative Commons: Attribution 4.0 (CC-BY)

Open Access

Tripathy, H. P. ORCID: <https://orcid.org/0000-0003-0129-2642>,
Pattanaik, P. ORCID: <https://orcid.org/0000-0002-0042-6672>,
Mishra, D. K. ORCID: <https://orcid.org/0000-0002-5648-8362>
and Holderbaum, W. ORCID: <https://orcid.org/0000-0002-1677-9624> (2023) Heat and moisture management for automatic air conditioning of a domestic household using FA-ZnO nanocomposite as smart sensing material. *Energies*, 16 (6). 2654. ISSN 1996-1073 doi: 10.3390/en16062654 Available at <https://centaur.reading.ac.uk/111341/>

It is advisable to refer to the publisher's version if you intend to cite from the work. See [Guidance on citing](#).

To link to this article DOI: <http://dx.doi.org/10.3390/en16062654>

Publisher: MDPI AG

copyright holders. Terms and conditions for use of this material are defined in the [End User Agreement](#).

www.reading.ac.uk/centaur

CentAUR

Central Archive at the University of Reading

Reading's research outputs online

Article

Heat and Moisture Management for Automatic Air Conditioning of a Domestic Household Using FA-ZnO Nanocomposite as Smart Sensing Material

Hara Prasada Tripathy ¹, Priyabrata Pattanaik ¹, Dilip Kumar Mishra ¹ and William Holderbaum ^{2,*}

¹ Semiconductor Research Laboratory, Faculty of Engineering and Technology (ITER), Siksha 'O' Anusandhan Deemed to be University, Bhubaneswar 751030, India; haraprasadtripathy@soa.ac.in (H.P.T.); priyabratapattanaik@soa.ac.in (P.P.)

² School of Biological Science, Biomedical Engineering, University of Reading, Reading RG6 6AY, UK

* Correspondence: w.holderbaum@reading.ac.uk

Abstract: Prior to the year 2000, air conditioning was not common in many cities throughout the world. However, today, 20 years later, air conditioning is common. This circumstance has a negative impact on the climate. Additionally, the situation regarding energy usage as a result of this is alarming. For a healthy and pleasant livelihood, indoor temperature and air flow must be controlled. False partitions with insulating layers have been used to regulate the temperature inside rooms, but they are unable to regulate the variation in humidity caused by the exchange of water between interior and exterior walls. In this manuscript, we provide a sensory system that can automatically detect relative humidity and temperature. Temperature is sensed at each layer of the false partition using an LM35-based integrated circuit and humidity is detected by an FA-ZnO nano-composite layer through an indoor false partition owing to changes in the material's resistance. Depending upon the change in resistance based on the fluctuation in temperature, the corresponding current responds by arduino microcontroller, and thus triggers the automated ON and OFF switch for air conditioning. Living and non-living bodies both lead pleasant and healthy lives when indoor units are managed properly.

Keywords: humidity sensor; moisture storage function; COMSOL multiphysics; four-probe method



Citation: Tripathy, H.P.; Pattanaik, P.; Mishra, D.K.; Holderbaum, W. Heat and Moisture Management for Automatic Air Conditioning of a Domestic Household Using FA-ZnO Nanocomposite as Smart Sensing Material. *Energies* **2023**, *16*, 2654. <https://doi.org/10.3390/en16062654>

Academic Editors: Katarzyna Ratajczak and Małgorzata Basińska

Received: 27 November 2022

Revised: 15 February 2023

Accepted: 8 March 2023

Published: 11 March 2023



Copyright: © 2023 by the authors. Licensee MDPI, Basel, Switzerland. This article is an open access article distributed under the terms and conditions of the Creative Commons Attribution (CC BY) license (<https://creativecommons.org/licenses/by/4.0/>).

1. Introduction

Rapid growth of a civilization has adverse effects on the environment, some of which are caused by deforestation and the dumping of water body. This may be the primary cause of long-term shifts in temperatures and weather patterns. These movements may be natural, but human activity has been the primary cause of climate change since the 1800s, mostly owing to the combustion of fossil fuels (such as coal, oil, and gas), which creates heat-trapping gases. Almost all geographical regions are experiencing an increase in hot days and heat waves. The year 2020 was one of the warmest years on record. Heat-related diseases become more common as temperatures rise, making it more difficult to work and move around. An elevated environmental temperature leads to an increase in heat and humidity. According to the Environmental Protection Agency (EPA), the optimal range for indoor relative humidity lies between 30% and 50%. Mold and material damage are reduced if building sites stay within this temperature range. Different construction designs have been adopted to protect structures from both the outside and the inside [1,2]. It is vital to note here that humidity and condensation do not constitute dampness. Instead, it is the repeated accumulation of humidity and condensation in the same location that can lead to the appearance of dampness. Dampness on walls creates unhygienic conditions for both living and nonliving bodies [3–6]. Indoor humidity levels are directly related to physical health and construction stability. Healthy environmental conditioning is only possible by both creating and controlling it. The main concern here is the side effects on human

health. Healthy environmental conditioning can be possible with the adaptation of the traditional/natural habitat or with controlled deforestation/urbanization. In order to have good air quality inside the house, the management of heat and moisture at appropriate levels throughout the year is essential [7–9]. One cannot create a natural climate that is exactly like nature itself, but it can be managed by controlling air conditioning units, for which different sensors have been created and implemented in different smart system integrations. These types of integrations are complicated and the failure of one can cause serious data interpretation. Energy loss due to the use of a larger system is an additional issue. The idea of green building has gained popularity over the past 10 years, and more people are becoming aware of its potential environmental advantages over more traditional building methods. Green building places a great emphasis on lowering energy consumption (via greater insulation, more energy-efficient appliances, and HVAC systems) as well as lowering the negative effects on human health and the environment [10]. Designing and creating low-energy structures as well as utilizing recycled or environmentally friendly materials are current trends in civil engineering [10]. In this context, investigations are being conducted to better understand and describe the hygrothermal performance and durability of novel recycled composites that are being developed [11]. Among building materials, wooden-based products appear to have interesting hygrothermal properties. Several researchers have aimed to determine the effectiveness of metamodels in forecasting building reactions [11–14]. Moreover, researchers are working on rammed earth folk house [15], construction and demolition waste [16], recycled expanded-polystyrene-based mortar [2], and hemp and stone wool insulations [1], among others. The purpose of this research work is to develop a composite material [17] for a wood-frame wall structure's interior wall, as well as a sensing material.

Researchers have been working to develop smart concrete composites to protect constructions as well as maintain the health of living and non-living bodies. Researchers are still working on the development of smart concrete composites to protect constructions [18–20], which will also help in controlling room temperature, moisture, and so on, mitigating any damage to non-living things or the health of human beings. The proposed work is a simulation study using ZnO–fly ash composite as a smart sensing material. The simulation work was carried out using COMSOL multiphysics software. The simulated environment performance analysis is based on thermal and hygric simulation [21]. It is predictable that hygrothermal simulations can help in analyses of the overall performance of buildings [10,11,14,22]. This study investigates the hygrothermal performance of building components, which are the fly ash–ZnO nano composite as the interior sensing layer of relative humidity, cellulose phase change material as the insulation layer with wood supporting the partition board, and concrete wall structures verifying the humidity level in the various building layers. The remainder of this paper includes the background of the study with proper justification for finding day-to-day problems, with a proper simulation design proposed, followed by the results and discussions. The data acquisition system with the overall instrumentation and control of the proposed research work is depicted.

2. Proposed Model Design

The hygrothermal simulation model for a domestic house with a core brick wall, concrete roof, and floor is described in this section. Figure 1 depicts the schematic diagram of the proposed design model. In this figure, the brick wall has covered with false partition and the false partition has three layers from outside to inside naming as: oriented standard board (OSB), compressed wood strands (flakes) and cellulose material based insulation layer. The third layer or the interior layer is made up off fly ash-ZnO nano composite based sensing material layer. The OSB is fabricated in the form of wide mats from cross-oriented layers of different wooden strips. They are compressed and bound together with wax and synthetic adhesive resin (95% wood, 5% resin, and wax). For insulation of the building from heat, thermal conductivity was employed using a wood and cellulose mixed insulation layer. This helps to reduce heat loss in the building.

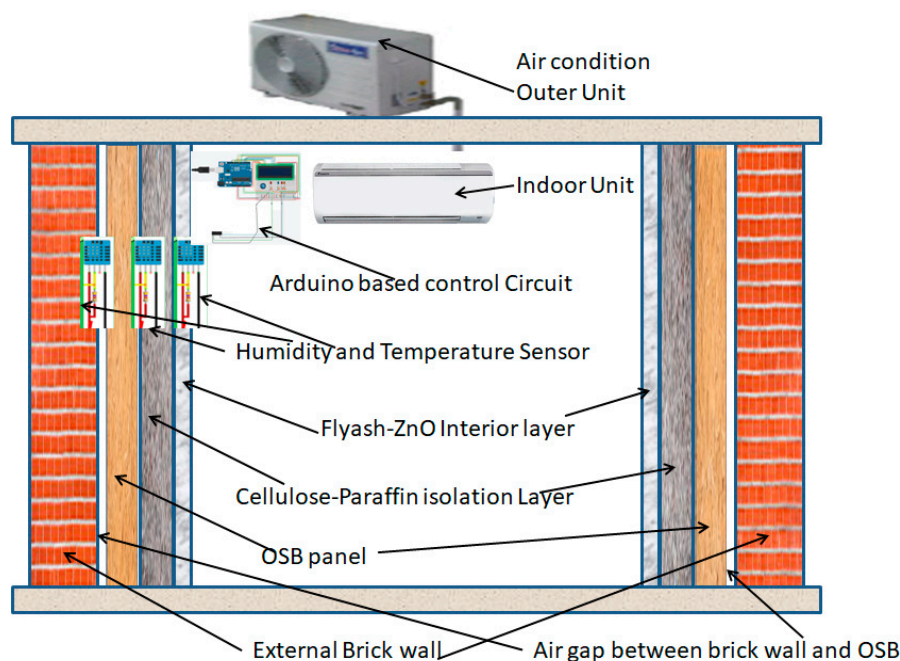


Figure 1. Proposed schematic diagram of the entire research work.

The sensing material layer is proposed here to accurately sense the humidity, and LM35 can be implemented to sense the temperature at various layers of the model. The popular temperature sensor series LM35 is a precise integrated circuit (IC) whose output voltage linearly proportional to centigrade temperature. These are having advantage over conventional linear temperature sensors calibrated in kelvin, as the users are not needed to substrate huge amount of constant voltage from the output for obtaining convenient centigrade scaling. LM35 sensor does not require any external trimming or calibration. The typical accuracies of these sensors for room temperature and elevated temperature ($-55\text{ }^{\circ}\text{C}$ to $150\text{ }^{\circ}\text{C}$) are $\pm 0.25\text{ }^{\circ}\text{C}$ and $\pm 0.75\text{ }^{\circ}\text{C}$ respectively. The liner output, precise inherent calibration and low-output impedance of LM35 device makes interfacing to control circuit especially easy. As like temperature sensor, copper plates are used to sense humidity. These plates are adjusted as 4 probe resistance method. The change in humidity has an effect on the electrical resistance. The change in resistance due to the change in humidity at a constant supplied DC voltage results in current. The resulting current is used to control the ON or OFF condition of the arduino circuit with the AC compressor. This research work is divided into two parts. Primarily, the hygrothermal simulation model is designed using COMSOL Multiphysics[®] 6.0, after which we propose a schematic model where LM35 temperature sensors are used with an arduino microcontroller to control AC. The sensing and circuitry details are depicted in later sections of the article.

The hygrothermal simulation model using COMSOL Multiphysics[®] [22]: COMSOL Multiphysics[®] software is used by engineers and scientists to simulate designs, devices, and processes in all disciplines of engineering, manufacturing, and scientific research. COMSOL Multiphysics[®] is a simulation platform that allows for both fully linked multiphysics and single-physics modeling. The Model Builder encompasses all of the modeling workflow phases, such as establishing geometry, material characteristics, and the physics that explain specific phenomena, as well as solving and post-processing models to obtain correct results. Figure 2 represents a portion of two-dimensional models with width and thicknesses of 0.8 m and 0.1475 m, respectively. The geometrical descriptions of each component are as follows. In the figure, the exterior and interior panels have thicknesses of 0.0125 m and 0.015 m, respectively. The exterior and interior panels are separated by two pine wood studs with a width of 0.045 m and height of 0.12 m. Three isolation boards made of cellulose

are placed between the wood frame. In the wall-frame structure, cellulose is used as a filler material to fill the various cavities.

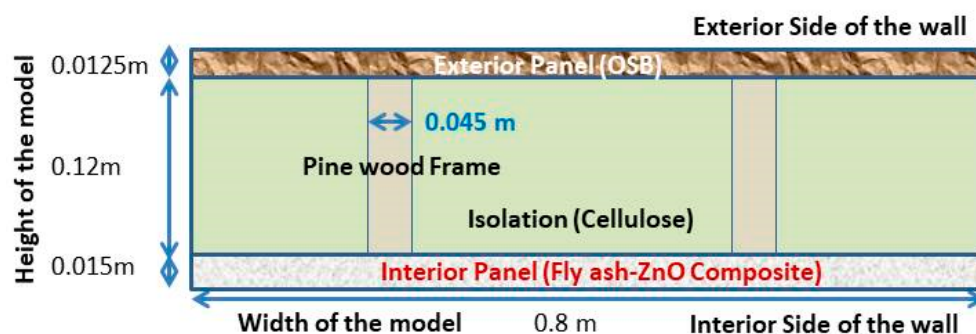


Figure 2. Two-dimensional hygrothermal model using COMSOL.

Wall structure: Under a given climatic condition, the moisture performance of the wall construction system is over-reliant on the system consonance, as well as the thermal and moisture characteristics of the constituent elements. Under Indian climatic conditions, moisture characteristics of wood and concrete wall structures are scrutinized. The exterior wall is a brick wall made of cement. The false wall is made of pine-wood-based OSB attached to the conventional brick wall. The isolation board is made from cellulose, with a bracing made of a wooden panel and interior siding made of fly ash–ZnO composite.

Weather condition and modeling parameter description: Convective moisture and heat flux surroundings are applied on the top and bottom margins to model the indoor and outdoor air flows next to the wall. The outdoor and indoor heat transfer coefficients are set as $h_{ext} = 25 \text{ W}/(\text{m}\cdot\text{K})$ and $h_{int} = 8 \text{ W}/(\text{m}\cdot\text{K})$, respectively. The outdoor and indoor moisture transfer coefficients are set to $\beta_{ext} = 25 \times 10^{-8} \text{ s}/\text{m}$ and $\beta_{int} = 8 \times 10^{-8} \text{ s}/\text{m}$, respectively, according to the correlation of the heat and mass transfer boundary layers. The side boundaries are designed for complete isolation in terms of heat and moisture. The indoor climatic situation is based on EN 13788. This comprises the high moisture load profile of buildings.

Dynamic modeling of heat and moisture transport: The idea behind this hygrothermal study is to analyze the moisture performance of buildings. This study is carried out using dynamic modeling of the transport of heat and moisture. Through this approach, both transport of liquid moisture by capillary forces and transport of vapor by diffusion are computed. Moreover, the latent heat effect due to vapor diffusion is modeled. In addition to the above, heat and moisture storage is also considered using moisture-dependent thermal properties.

Static modeling of heat and moisture transport [21]: By ignoring heat and moisture storage, the latent heat effect, and capillary transport of liquid moisture, the following equations are obtained for transport of heat and moisture. The Glaser method is developed to assess the moisture balance of a building component by considering the vapour diffusion transport process. The Glaser technique uses a simple calculation of the interstitial condensation level based on average monthly temperatures, vapour pressure, and steady-state heat conduction if critical condensation thresholds are achieved within one year. Glaser's [21,22] calculations are not a replica of reality, but rather a technique for determining the danger of interstitial condensation. The state of condensation was determined using the effective volumetric heat capacity at a constant pressure, effective thermal conductivity, temperature, latent heat of evaporation, vapour permeability, relative humidity, and vapour saturation pressure. Accordingly, moisture storage capacity and moisture diffusivity were determined. These equations are known as the Glaser method. They can be solved in the moisture transport in building materials interface by setting the moisture diffusivity to 0, as well as in the heat transfer in building materials interface by setting the vapor permeability to 0.

Modeling of the vapor barrier: Upside and downside moisture fluxes are defined and applied at the interface between the interior siding and the isolation board to model

the vapor barrier. The moisture transfer coefficient β is defined, where δ is the vapor permeability of still air (SI unit: s), P_{sat} is the saturation pressure of water vapor (SI unit: Pa), μ is the vapor resistance factor (dimensionless), and ds is the vapor barrier thickness (SI unit: m).

Evaluation of hygrothermal performance: The effect of boundary and exposure conditions: The relative humidity between the wall structure due to the variation in temperature plays a role in moisture buildup. The change in indoor temperature can cause an unusual temperature profile of the building construction material. The low temperature value leads to a higher moisture accumulation potential. Thus, it leads to condensation in the insulation layer during summer as well as when it is hotter outdoors than indoors. Basically, an air conditioning unit helps to lower the indoor temperature.

These analyses are performed with the consideration of leading a comfortable life through automatic control of moisture levels. This control also helps extend the life of construction materials. Using waste products like FA and converting them to FA-ZnO composites to be used as a sensing material is a rather challenging task. The research work was conducted. The results of the model are analyzed and discussed in the section following the data acquisition system and instrumentation section.

3. Data Acquisition System and Instrumentation

The data acquisition system with sensor integration for the proposed model is depicted in Figure 3a. In this research work, we propose a system comprises of four probe sensory system with proper isolation, false wall (OSB and wood-cellulose composite) coated with FA-ZnO sensing material (inner side of the wall), arduino microcontroller with power supply setup, three numbers of temperature sensor (LM35), four numbers of LED, one display unit respectively. At each layer, one LM35 is installed. For each unit change in the temperature, the corresponding LED indicates the change values. The change values are then displayed in the display section. Depending upon the resistance value, the humidity of the indoor unit sensed by the sensing layer and the corresponding current value triggers the automated switch for AC operation. The setup is designed such a way that the insulation, which absorbs the maximum amount of water droplets, can be automatically cooled down or heated up by the AC unit. This helps to maintain a comfortable and healthy living environment inside the home. The room temperature and humidity values are also monitored by the mobile app, as shown in Figure 3b. The temperature and humidity values are sent to the mobile through the SIM900A modem, Easy Electronics, India. SIM900A is a dual-band GSM or GPRS-based modem from SIMCOM. Its operating frequency is 900 or 1800 MHz with baud rate, which is configurable from 1200 to 115,200 through a programming command. The GSM or GPRS modem with internal TCP/IP stack enables the device to connect to the internet via GPRS. Once the SIM900A is connected to a power supply and an arduino controller, it automatically selects the operating frequency of 900 or 1800 MHz. The baud rate is set to 115,200. Once the internet connection is established, the data from the sensing device are transferred to the app, and the parameters are displayed on the mobile as shown in Figure 3. From the app, values of outside temperature, room temperature, and room humidity can be monitored. The setting and adjustment of the room temperature and room humidity, with fan speed and the ON or OFF condition of the AC compressor can performed remotely with the mobile app. The user can also turn the AC OFF or ON directly from the app

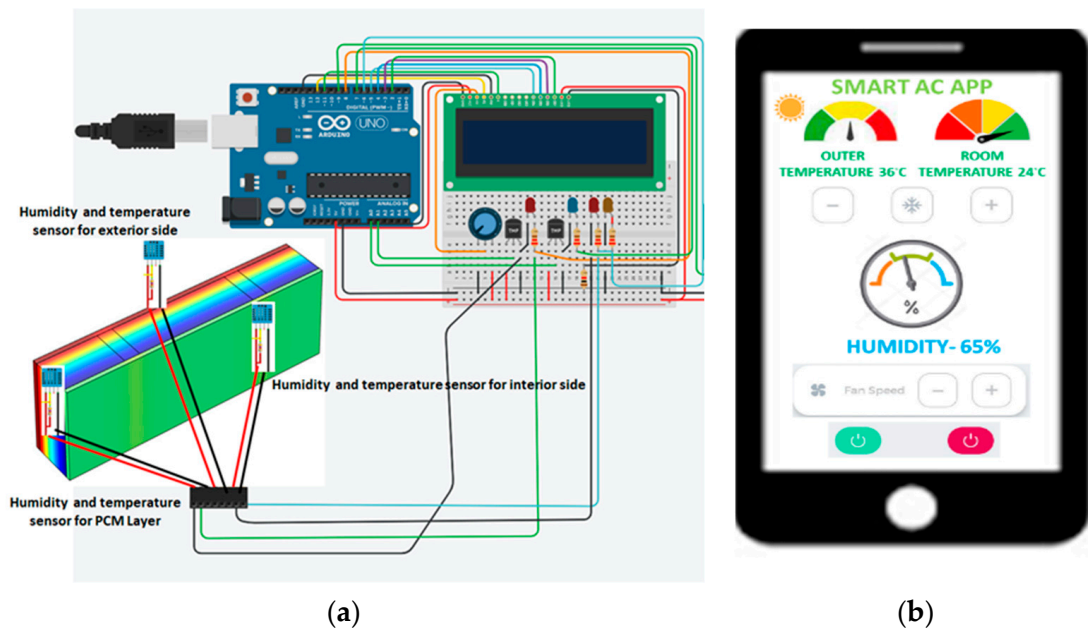


Figure 3. (a) Proposed data acquisition with sensor system integration; (b) implementable mobile app for smart AC.

4. Results and Discussions

4.1. Temperature Variation in the Model

The designed model is affected by temperature. The thermal conductivity is highly dependent on the water content and temperature. Figure 4a depicts the temperature variation from the outer side to the inner side of the wall. The temperatures in the OSB and sensing layer are 35 °C and 24 °C, respectively. The temperature change occurs as a result of the cellulose-based insulation layer. The COMSOL multiphysics proposed model clearly depicts the temperature variation at each point of the false partition.

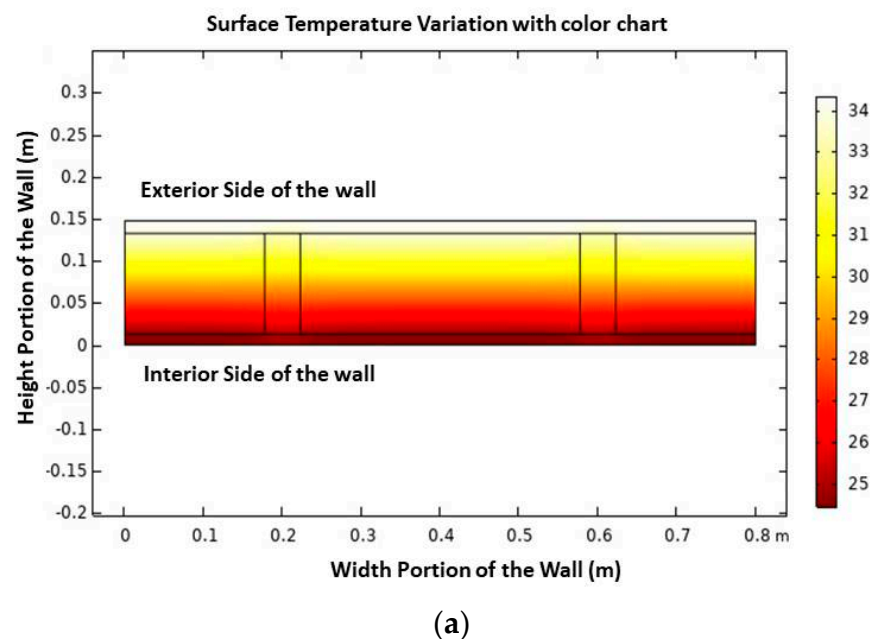


Figure 4. Cont.

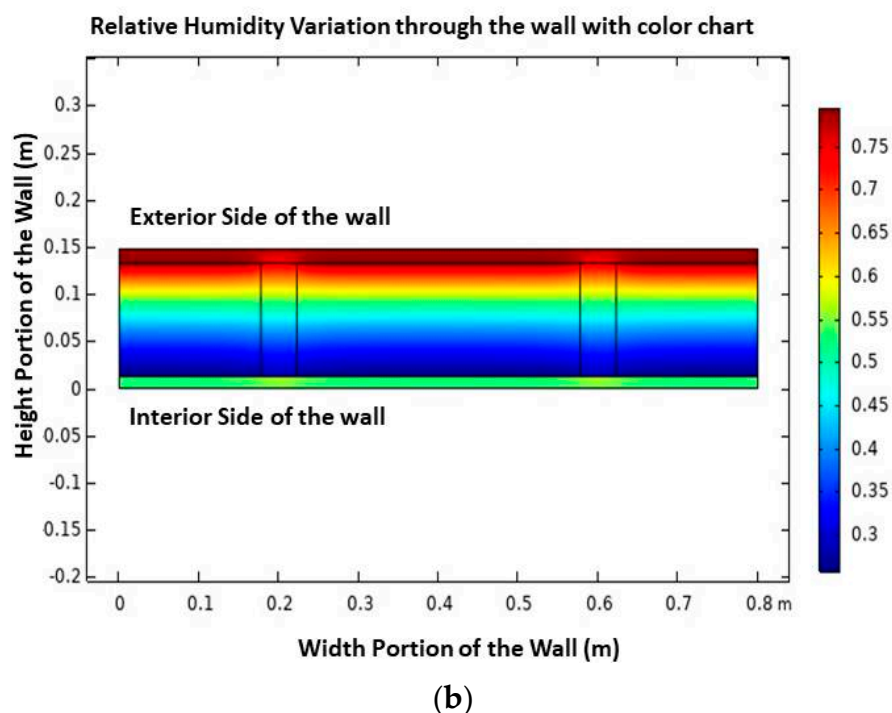


Figure 4. Two-dimensional cross-sectional view: (a) surface temperature variation and (b) relative humidity through the wall structure.

4.2. Relative Humidity

Figure 4b depicts the two-dimensional cross-sectional view of the model. The relative humidity of the sample on a normal summer day in India is shown in the pictorial view. The variation in humidity level from the exterior to interior portion of a domestic household is analyzed in the figure. The ideal humidity level to maintain a healthy and comfortable living environment is in the range of 0.3–0.5. The instrumentation is carried out to measure the humidity level at each layer of the construction in an accurate manner. In general, the humidity of biodegradable material is greater than 80%, which causes condensation. In this hygrothermal model, cellulose composite is used as thermal insulation layer of a building. These are in the form of rigid panels assembled on the building sites. Good phonic insulation helps protect the building from different impacts and airborne noises. However, to sense the relative humidity in each layered structure, we have proposed an experimental setup in which sensors are implemented to sense the temperature in each layer and coated sensing material is used to sense the relative humidity.

4.3. Moisture Storage Function

In a porous hygroscopic material, the surfaces of the pore system accumulate water molecules until reaching a specific equilibrium moisture content, corresponding to reaching the humidity of the ambient air. The moisture storage function (MSF) across the false partition of the wall is depicted in Figure 5. Owing to the insulation material layer, MSF changes rapidly between 0.065 m and 0.085 m from 43 kg/m³ to 41.2 kg/m³, and vice versa. The reversal of MSF may be caused by the insulation layer, thus a constant MSF value is maintained until the end of the false wall structure assembly. The total water content difference between the false partition frame and concrete wall structures is due to differences in the hygroscopicity of the materials that make up the different wall layers. The false partition frame wall structures contain wood elements, OSB, cellulose insulation, and fly ash–ZnO composite board along with the concrete wall structure. The use of OSB in the wood frame wall typically has an effect on the hourly variation in relative humidity. Both the moisture content and the water vapor saturation pressure play a vital role in adjusting

and maintaining the MSF profile at a constant value of 43 kg/m^3 with the change in temperature from $35 \text{ }^\circ\text{C}$ (outer layer) to $24 \text{ }^\circ\text{C}$ (inner layer) and change in relative humidity from 0.65 to 0.45. This is due to the different construction assemblies. OSB and cellulose have a high water storage capacity. Through this change, the MSF value becomes constant at 43 kg/cm^2 . For hygroscopic materials, a transient reduction in the heat and moisture buffer function is required to maintain temperatures for the protection of construction materials and human health.

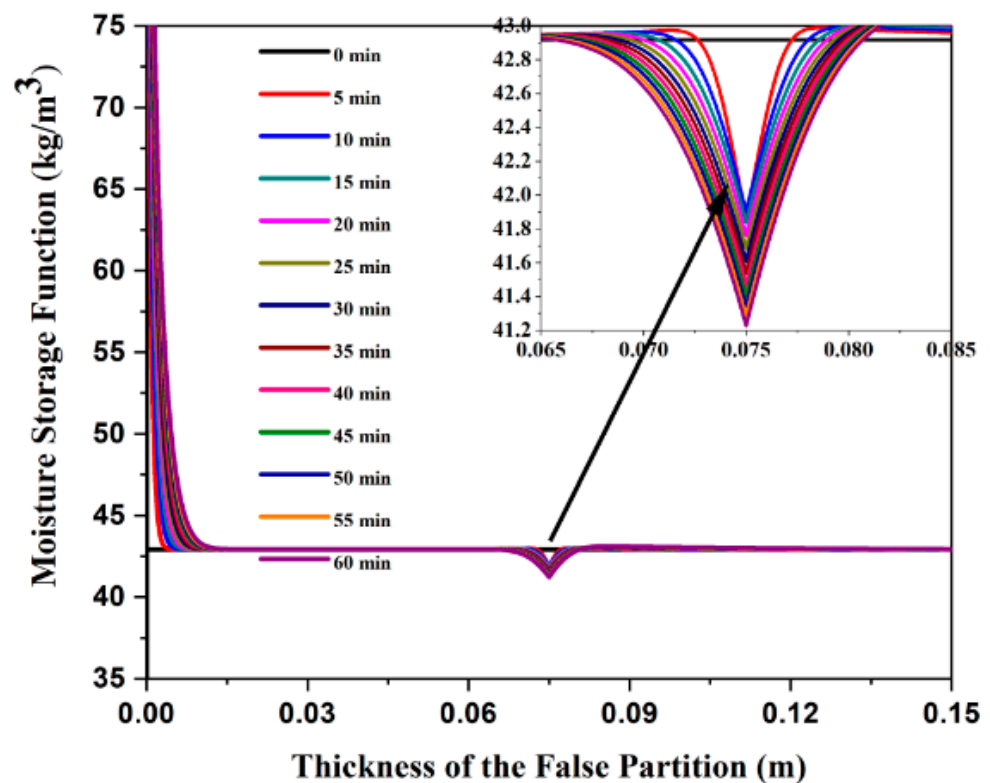


Figure 5. Moisture profile of the false partition.

4.4. Sensor Setup

To sense the change in humidity due to temperature, sensor arrangement is necessary for the protection of both construction elements and human health. The proposed fly ash (FA) and zinc oxide (ZnO) composite is used as an interior panel of the wood-frame wall to replace gypsum board. For the experimental setup, the proposed composite has undergone various processes to form a pallet-like structure. FA–ZnO powder was ground thoroughly using polyvinyl acetate (PVA). In this process, PVA acts as a binder. By applying 6 tons of pressure in the palletizer, the PVA was mixed with FA–ZnO powder for 8 min. Cylindrical-shaped pallets are then formed after the prescribed time. The cylindrical-shaped pallets are then ground using a micro sand grinding machine to form square-shaped plates. For testing purposes, FA–ZnO square sheets were used with a height of 0.003 m and area of 0.000078 m^2 , respectively. The resistivity (ρ) of the FA–ZnO composite was calculated using Equation (1).

$$\rho = \frac{V \cdot A}{I \cdot L} \quad (1)$$

The voltage reading [V], current reading [A], cross-sectional area [m^2], and distance between the inner electrodes [m] are denoted as V, I, A, and L, respectively. In this research work, a four-probe arrangement using copper plates was used to provide a 10 V DC supply to one pair. The four-probe method is used over the over two-probe method to avoid a glitch in the resistance value, which is depicted in Figure 6. The components for the experimental arrangements are a BK precision 4071A signal generator (Yorba Linda, CA,

USA), two channel Tektronix TDS 1002 oscilloscopes ($\pm 3\%$ accuracy) (Beaverton, OR, USA), a digital multimeter (Fluke, $\pm 1.2\%$ accuracy) (China) with a voltage supply of 10 V, and a frequency ranging from 1 to 100 kHz. The effective range of frequency for a multi meter is 10 kHz. The inner two copper electrodes are used to draw the voltage values, whereas the outer two plates are used to measure the AC current between foil electrodes. The resistance of the material at room temperature ($28\text{ }^{\circ}\text{C}$) and final elevated temperature of the environment ($48\text{ }^{\circ}\text{C}$) are $30.4 \times 10^6\ \Omega$ and $1.30 \times 10^6\ \Omega$, respectively, as shown in Figure 7. In this research work, the maximum fractional change in resistivity (FCR) is calculated as follows: $\text{FCR} = \frac{\rho_i - \rho_o}{\rho_o}$, where ρ_i and ρ_o are readings of electrical resistivity measured at the initial stage and during the operational stage, respectively. At room temperature ($28\text{ }^{\circ}\text{C}$) and the final elevated temperature ($48\text{ }^{\circ}\text{C}$), the resistivity of the proposed sample is $797.0 \times 10^3\ \text{ohm}\cdot\text{m}$ and $34.1 \times 10^3\ \text{ohm}\cdot\text{m}$, respectively.

FA-ZnO Sensing Layer

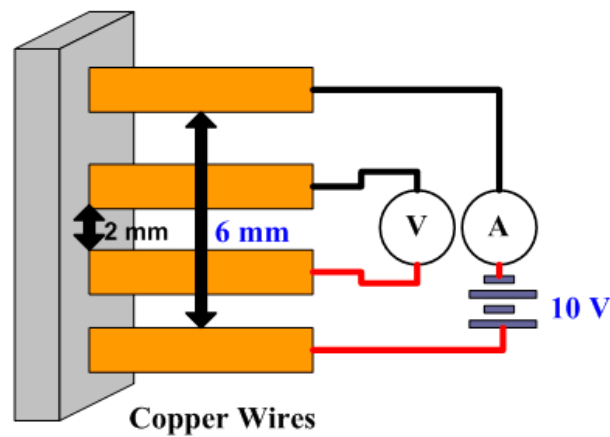


Figure 6. Sensor setup using the four-probe method.

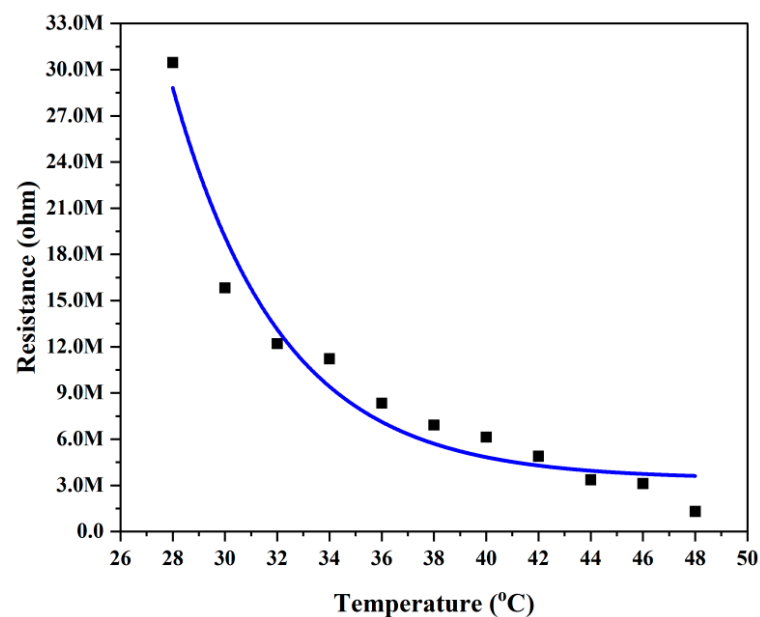


Figure 7. Role of resistance due to the increase in environmental temperature.

The maximum fractional change in resistivity of the material is 22.37. The temperature, resistivity, and resistance of the sample are measured successfully, but the relative humidity of the sample can only be measured by the analog hygrometer implemented on the FA-ZnO

sensing layer. The corroboration with environmental temperature is depicted in Figure 8. It shows that the increase in temperature increases the relative humidity by decreasing the resistance value of the sample, as depicted in Figure 9. The resistance is measured continuously using an arduino microcontrolling unit. The change in relative humidity base value from 0.25 to 0.75 is monitored experimentally using FA–ZnO composite as sensing material. For composite samples, as the resistance value lies between $M\Omega$, it can be measured with an LCR meter. The output data values from both the proposed FA–ZnO nano-composite-based humidity sensor and commercially available analog humidity sensor are corroborated and depicted in Figure 10. In the Figure 10, we have used two sets of data likely proposed and available humidity sensor values. The data values of proposed humidity sensor are having a correlation value of 0.9995 with commercial humidity sensor. The sensor values both proposed and commercial are not only correlated but also verified their distribution over large sensing range. The mean and standard deviation between proposed and available humidity sensors are 42.89 ± 18.3 and 42.81 ± 18.5 , respectively. The large standard deviation is the feature of the quite spread-out data, which is observed due to the large variation of temperature value (i.e., from 35°C of outer wall to 28°C on inner wall) as moving from the outer wall to inner wall.

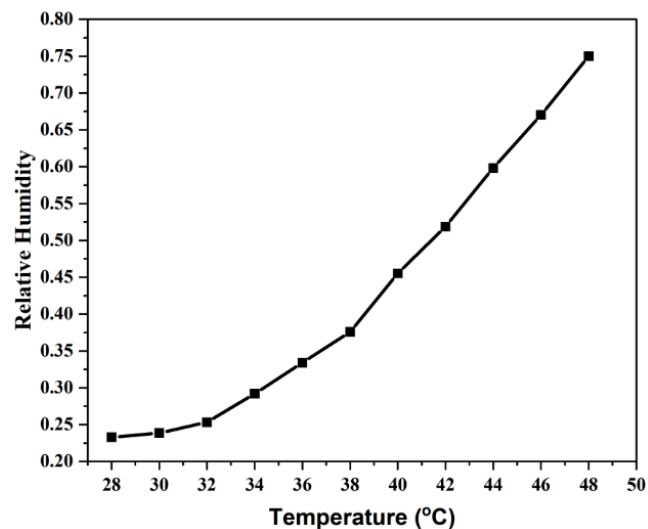


Figure 8. Corroboration between LM35 and hygrothermal data values.

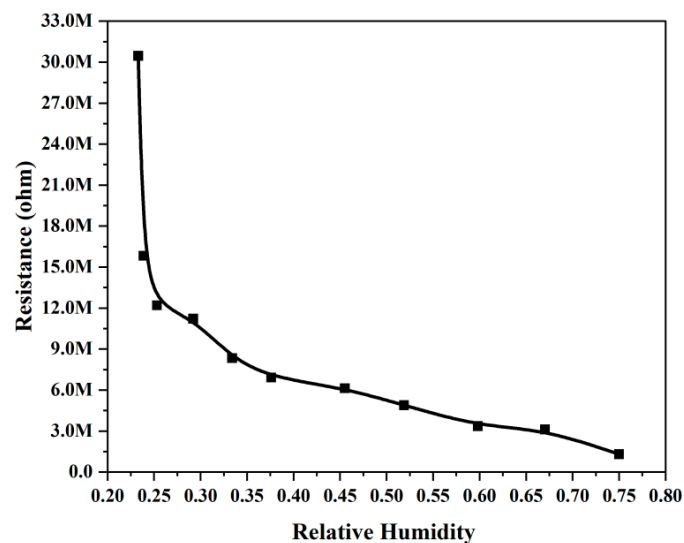


Figure 9. Environmental relative humidity vs. resistance of the FA–ZnO sensing material.

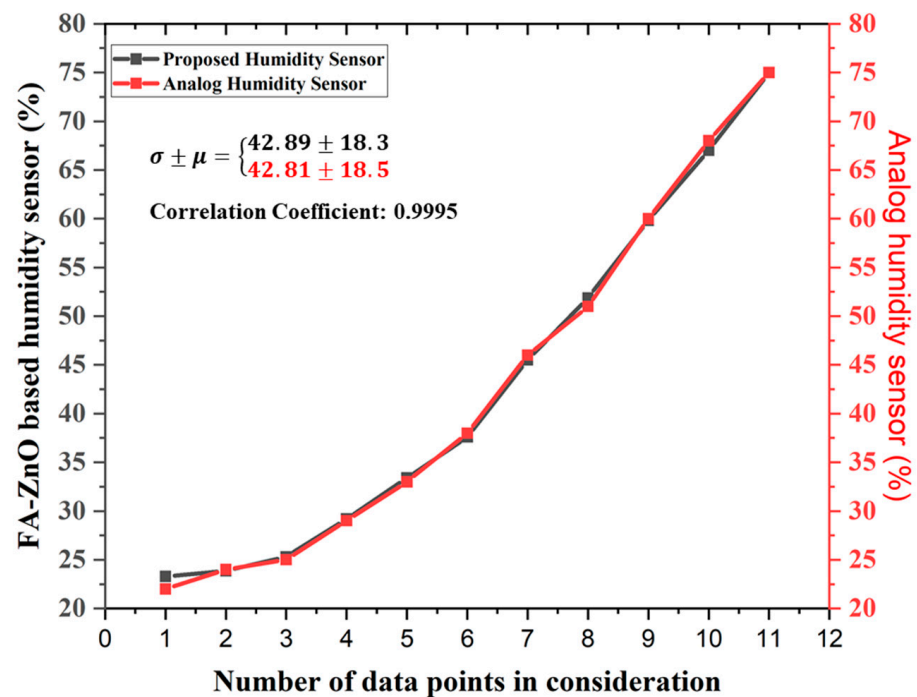


Figure 10. Validation of the proposed sensor by corroboration with the commercial analog humidity sensor.

5. Conclusions

In this paper, hygrothermal modeling is carried out using COMSOL multiphysics. False partition including an insulation layer can help an indoor unit to cool down by restricting the radiation of heat. Both the moisture content and the water vapor saturation pressure play a vital role in adjusting and maintaining the MSF profile at a constant value of 43 kg/m^3 with the change in temperature from $35 \text{ }^\circ\text{C}$ (outer layer) to $24 \text{ }^\circ\text{C}$ (inner layer) and change in relative humidity from 0.65 to 0.45. This is due to the different construction assemblies. LM35 can be implemented to sense temperature at various layers of the model and an FA–ZnO nano composite sensing material layer is proposed here to accurately sense humidity. The mean and standard deviation between the proposed and available humidity sensors are 42.89 ± 18.3 and 42.81 ± 18.5 , respectively. The data values of the proposed humidity sensor have a correlation value of 0.9995 with the commercial humidity sensor. Realization of this research on a larger scale can involve a new generation sensing mechanism with maintaining adequate conditions for a healthy life for both living and non-living bodies.

Author Contributions: H.P.T.: Conceptualization, Validation, Data Curation; P.P.: Conceptualization, Software, Data Curation; D.K.M.: Formal Analysis and Editing; W.H.: Supervision. All authors have read and agreed to the published version of the manuscript.

Funding: This research received no external funding.

Institutional Review Board Statement: Not applicable.

Informed Consent Statement: Not applicable.

Data Availability Statement: Data sharing not applicable.

Conflicts of Interest: The authors declare no conflict of interest.

References

1. Latif, E.; Ciupala, M.A.; Wijeyesekera, D.C. The comparative in situ hygrothermal performance of Hemp and Stone Wool insulations in vapour open timber frame wall panels. *Constr. Build. Mater.* **2014**, *73*, 205–213. [CrossRef]
2. Maaroufi, M.; Belarbi, R.; Abahri, K.; Benmahiddine, F. Full characterization of hygrothermal, mechanical and morphological properties of a recycled expanded polystyrene-based mortar. *Constr. Build. Mater.* **2021**, *301*, 124310. [CrossRef]
3. Kifer, D.; Sulyok, M.; Jakšić, D.; Krska, R.; Šegvić Klarić, M. Fungi and their metabolites in grain from individual households in Croatia. *Food Addit. Contam. Part B Surveill.* **2021**, *14*, 98–109. [CrossRef] [PubMed]
4. Radeef, H.R.; Abdul Hassan, N.; Zainal Abidin, A.R.; Mahmud, M.Z.H.; Yaacob, H.; Mashros, N.; Mohamed, A. Effect of aging and moisture damage on the cracking resistance of rubberized asphalt mixture. *Mater. Today Proc.* **2021**, *42*, 2853–2858. [CrossRef]
5. Eckelman, C.A. The Shrinking and Swelling of Wood and Its Effect on Furniture. *Forestry* **1998**, *1–26*, 1.
6. Sam-Daliri, O.; Faller, L.-M.; Farahani, M.; Zangl, H. Structural health monitoring of adhesive joints under pure mode I loading using the electrical impedance measurement. *Eng. Fract. Mech.* **2021**, *245*, 107585. [CrossRef]
7. Axelrad, R. Indoor Air Quality. In *Safe and Healthy School Environments*; Springer: Singapore, 2009; pp. 69–73. ISBN 9780199864638.
8. Corlan, R.V.; Balogh, R.M.; Ionel, I.; Kilyeny, S. The importance of indoor air quality. *J. Phys. Conf. Ser.* **2010**, *1781*, 2010. [CrossRef]
9. Cincinelli, A.; Martellini, T. Indoor air quality and health. *Int. J. Environ. Res. Public Health* **2017**, *14*, 1286. [CrossRef] [PubMed]
10. Aggarwal, C.; Ge, H.; Defo, M.; Lacasse, M.A. Hygrothermal performance assessment of wood frame walls under historical and future climates using partial least squares regression. *Build. Environ.* **2022**, *223*, 109501. [CrossRef]
11. Freire, R.Z.; Dos Santos, G.H.; Dos Santos Coelho, L. Hygrothermal dynamic and mould growth risk predictions for concrete tiles by using Least Squares Support Vector Machines. *Energies* **2017**, *10*, 1093. [CrossRef]
12. Marincioni, V.; Marra, G.; Altamirano-Medina, H. Development of predictive models for the probabilistic moisture risk assessment of internal wall insulation. *Build. Environ.* **2018**, *137*, 257–267. [CrossRef]
13. Van Gelder, L.; Das, P.; Janssen, H.; Roels, S. Comparative study of metamodelling techniques in building energy simulation: Guidelines for practitioners. *Simul. Model. Pract. Theory* **2014**, *49*, 245–257. [CrossRef]
14. Tijsskens, A.; Roels, S.; Janssen, H. Neural networks for metamodelling the hygrothermal behaviour of building components. *Build. Environ.* **2019**, *162*, 106282. [CrossRef]
15. Gao, Q.; Wu, T.; Liu, L.; Yao, Y.; Jiang, B. Prediction of Wall and Indoor Hygrothermal Properties of Rammed Earth Folk House in Northwest Sichuan. *Energies* **2022**, *15*, 1936. [CrossRef]
16. Bagarić, M.; Banjad Pečur, I.; Milovanović, B. Hygrothermal performance of ventilated prefabricated sandwich wall panel from recycled construction and demolition waste—A case study. *Energy Build.* **2020**, *206*, 109573. [CrossRef]
17. Panda, S.S.; Tripathy, H.P.; Pattanaik, P.; Mishra, D.K.; Kamilla, S.K.; Khandual, A.; Holderbaum, W.; Sherwood, R.; Hawkins, G.; Masakapalli, S.K. Structural, Morphological, Optical and Electrical Characterization of Gahnite Ferroan Nano Composite Derived from Fly Ash Silica and ZnO Mixture. *Materials* **2022**, *15*, 1388. [CrossRef] [PubMed]
18. Zhu, G.; Luo, Y.; Tang, J.; Han, N.; Xing, F. Preparation of biocompatible and water-proof microcapsule for self-healing concrete. In Proceedings of the Fifth International Conference on Self-Healing Materials, Durham, NC, USA, 22–24 June 2015; pp. 2–5.
19. Xiao, Z.; Liu, L.H.; Liu, T.; Yang, D.; Jia, X.; Du, Y.K.; Li, S.Q.; Yang, W.J.; Xi, Y.M.; Zeng, R.C. Degradation and biocompatibility of genipin crosslinked polyelectrolyte films on biomedical magnesium alloy via layer-by-layer assembly. *Prog. Org. Coat.* **2023**, *175*, 107372. [CrossRef]
20. Sarcinella, A.; Frigione, M. Sustainable and Bio-Based Coatings as Actual or Potential Treatments to Protect and Preserve Concrete. *Coatings* **2022**, *13*, 44. [CrossRef]
21. COMSOL Multiphysics. *Condensation Risk in a Wood-Frame Wall*; COMSOL Inc.: Burlington, MA, USA, 2017; pp. 1–36. Available online: https://doc.comsol.com/5.6/doc/com.comsol.help.models.porous.wood_frame_wall/models.porous.wood_frame_wall.pdf (accessed on 26 November 2022).
22. Knarucd, J.I.; Geving, S. Implementation and benchmarking of a 3D hygrothermal model in the COMSOL Multiphysics software. *Energy Procedia* **2015**, *78*, 3440–3445. [CrossRef]

Disclaimer/Publisher’s Note: The statements, opinions and data contained in all publications are solely those of the individual author(s) and contributor(s) and not of MDPI and/or the editor(s). MDPI and/or the editor(s) disclaim responsibility for any injury to people or property resulting from any ideas, methods, instructions or products referred to in the content.